

Supplementary Information

**Solid (cyanomethyl)trimethylammonium salts for electrochemically stable electrolytes
for lithium metal batteries**

Ruhamah Yunis,^a Jennifer M. Pringle,^a Xiaoen Wang,^a Gaetan M. A. Girard,^a Robert Kerr,^a Haijin Zhu,^b Patrick C Howlett,^a Douglas R. MacFarlane,^c Maria Forsyth^{a,*}

^aInstitute for Frontier Materials (IFM), Deakin University, Burwood, Victoria 3125, Australia

^bInstitute for Frontier Materials, Deakin University, Geelong, VIC 3217, Australia

^cSchool of Chemistry, Monash University, Wellington Road, Clayton, VIC 3800, Australia.

*Email: maria.forsyth@deakin.edu.au; jenny.pringle@deakin.edu.au

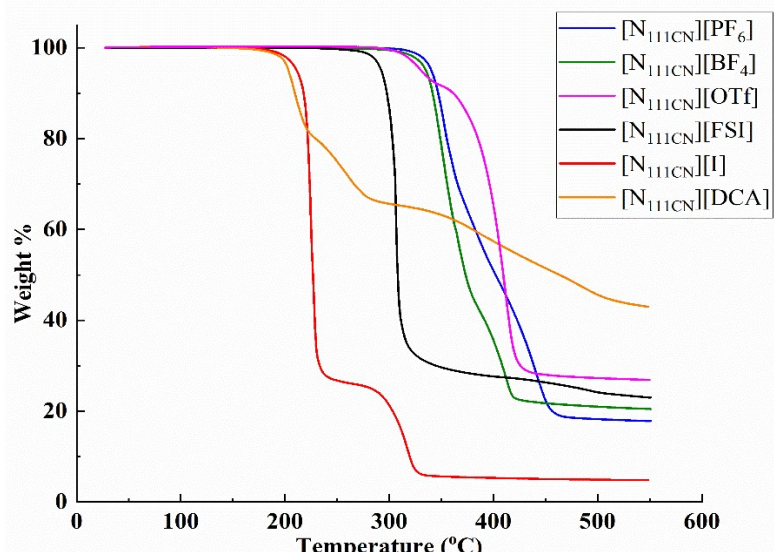


Figure S1. TGA curve for the cyano-ammonium salts

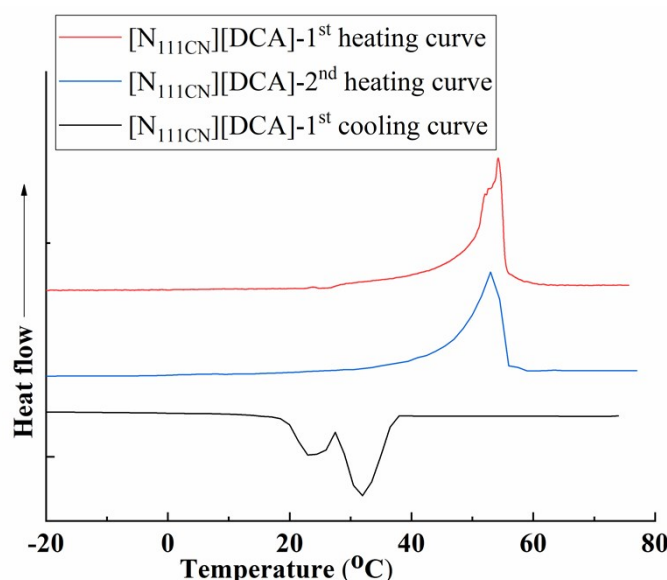


Figure S2. DSC for [N₁₁₁CN][DCA] at 2 °C /min as heating run. This is taken as first heating (2 °C /min) and first cooling curve (10 °C/min). A small shoulder appears

during first heating curve with melting peak, while during cooling cycle two crystallization peaks appear. The sample was held at low temperatures for an hour before heating was performed.

Table S1; Ionic conductivities and activation energies (E_a) for $[\text{N}_{111}\text{CN}]^+$ salts

	Conductivity (S cm ⁻¹ at 30 °C)	E_a (k J mol ⁻¹)
$[\text{N}_{111}\text{CN}]\text{[DCA]}$	3.2×10^{-6}	38 (Melt)
$[\text{N}_{111}\text{CN}]\text{[FSI]}$	2.1×10^{-8}	58 (phase I)
$[\text{N}_{111}\text{CN}]\text{[OTf]}$	6.7×10^{-9}	118 (phase I)
$[\text{N}_{111}\text{CN}]\text{[BF}_4\text{]}$	6.6×10^{-8}	53 (phase I)
$[\text{N}_{111}\text{CN}]\text{[PF}_6\text{]}$	7.2×10^{-10}	63 (phase I)
$[\text{N}_{111}\text{CN}]\text{[NTf}_2\text{]}^1$	10 ⁻⁴ at room temperature	---
$[\text{N}_{111}\text{CN}]\text{[CPFSA]}^2$	10^{-7} at 60 °C	---

The activation energy was calculated from the ionic conductivity data for $[\text{N}_{111}\text{CN}]\text{[DCA]}$, $[\text{N}_{111}\text{CN}]\text{[FSI]}$, $[\text{N}_{111}\text{CN}]\text{[OTf]}$, $[\text{N}_{111}\text{CN}]\text{[BF}_4\text{]}$ and $[\text{N}_{111}\text{CN}]\text{[PF}_6\text{]}$ (Table S1). Except for $[\text{N}_{111}\text{CN}]\text{[DCA]}$, all activation energies are for phase I. The lowest activation energy is seen for $[\text{N}_{111}\text{CN}]\text{[DCA]}$ because it is in a liquid state. The lowest activation energy in the solid phase I is seen for $[\text{N}_{111}\text{CN}]\text{[BF}_4\text{]}$, which is consistent with the greater disorder and higher conductivity compared to the other cyano-ammonium salts.

Table S2: DSC data and ionic conductivities (σ) for lithium-based electrolyte solutions.
Phase transition temperatures includes, glass transition temperature = T_g , solid-solid transitions = T_{s-s} and melting temperature = T_m and are taken as onset (otherwise specified as peak). The entropy change (ΔS) is also calculated for T_{s-s} and T_m .

	T_g (°C)	$T_{s-s} \pm 1$ (°C)	$\Delta S \pm 10\%$ (J K ⁻¹ mol ⁻¹)	$T_{s-s} \pm 1$ (°C)	$\Delta S^b \pm 10\%$ (J K ⁻¹ mol ⁻¹)	$T_m \pm 1$ (°C)	$\Delta S^b \pm 10\%$ (J K ⁻¹ mol ⁻¹)	σ (S cm ⁻¹)
10 mol% LiFSI in $[\text{N}_{111}\text{CN}]\text{[FSI]}$				-68	5	72	45	2.5×10^{-5}
50 mol% LiFSI in $[\text{N}_{111}\text{CN}]\text{[FSI]}$	-54							0.98×10^{-3}
10 mol% LiBF₄ in $[\text{N}_{111}\text{CN}]\text{[BF}_4\text{]}$		-61	11	77	0.3			2.5×10^{-7}
50 mol% LiBF₄ in $[\text{N}_{111}\text{CN}]\text{[BF}_4\text{]}$		53	3	79	11	112 broad melt (taken)		3.1×10^{-7}

						as peak)		
--	--	--	--	--	--	-------------	--	--

Table S3: Activation energies (E_a) (from ionic conductivities) and glass transition temperatures (T_g) for 50 mol% LiFSI-based liquid electrolytes. IL = ionic liquid and OIPC = organic ionic plastic crystal

OIPC or IL	E_a (kJ mol ⁻¹)	T_g (°C)
[C ₂ mpyr][FSI] ³ (OIPC)	31	-81
[C ₂ epyr][FSI] ⁴ (OIPC)	27	-75
[C ₃ mpyr][FSI] ⁵ (IL)	27	-73
[P _{111i4}][FSI] ⁶ (IL)	33	-71
[C _(i3) mpyr][FSI] ⁷ (OIPC)	28	-69
[N _{111CN}][FSI] (organic salt)	36	-54

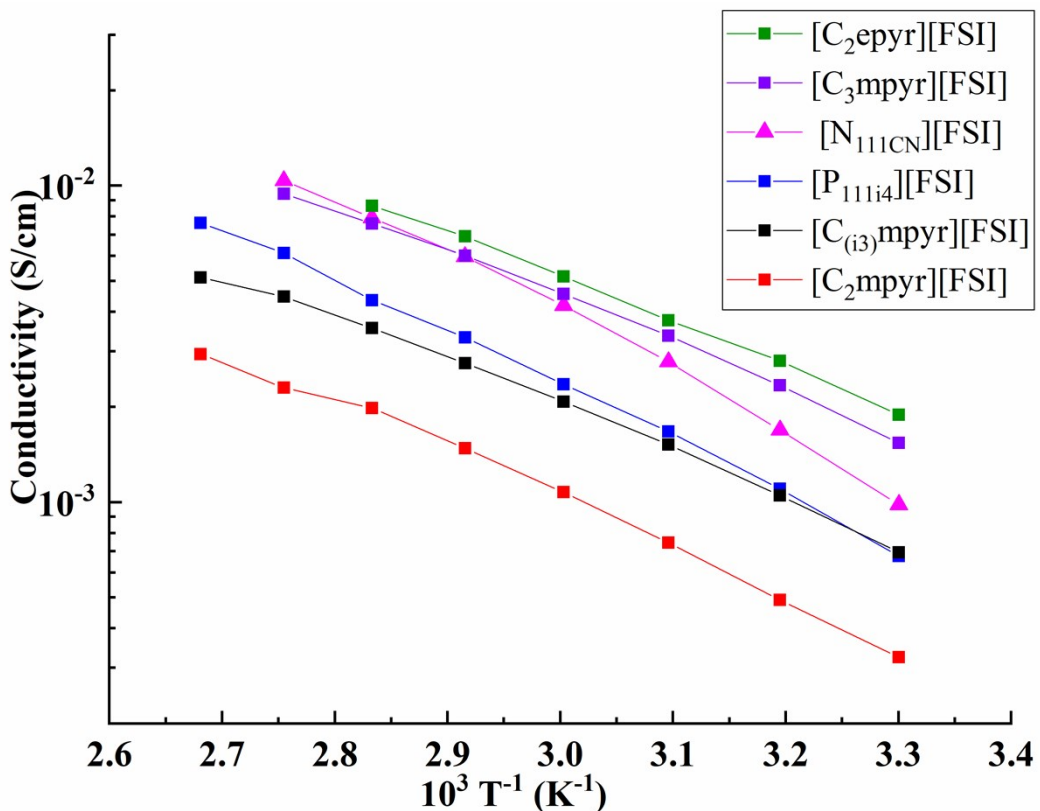


Figure S3. Comparison of conductivity plot of 50 mol% LiFSI-based liquid electrolytes in different OIPCs ([C₂epyr][FSI],⁴ [C₂mpyr][FSI]³ and [C_(i3)mpyr][FSI]⁷) and ILs ([C₃mpyr][FSI]⁸ and [P_{111i4}][FSI]⁹).

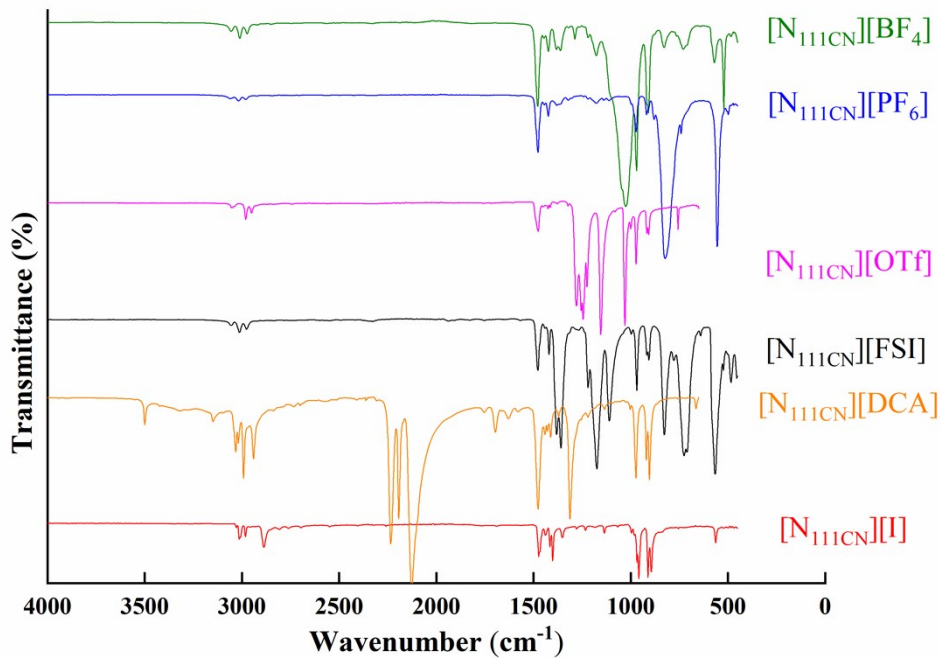


Figure S4. FTIR spectra for synthesized cyano-ammonium salts. Y-axis was adjusted for clarity.

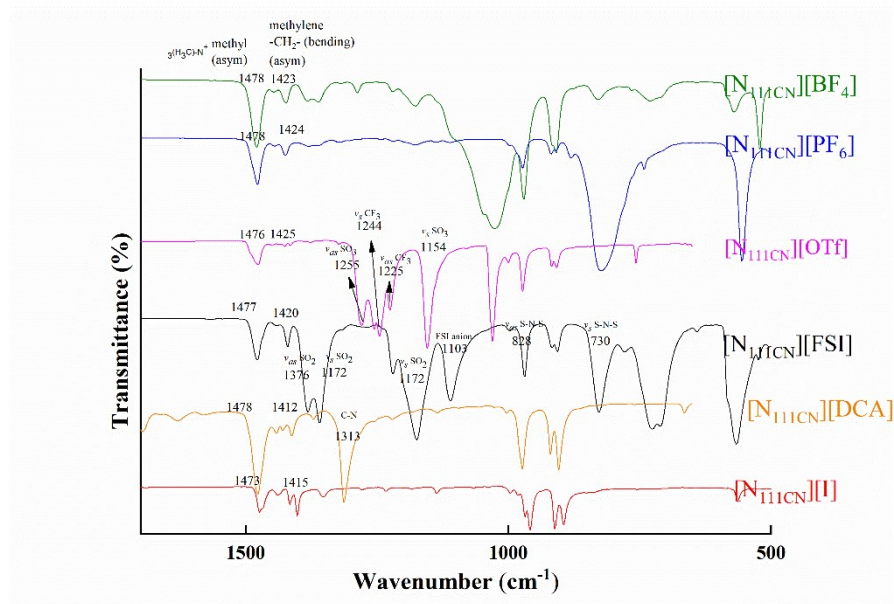


Figure S5. FTIR spectra for synthesized cyano-ammonium salts. Y-axis was adjusted for clarity.

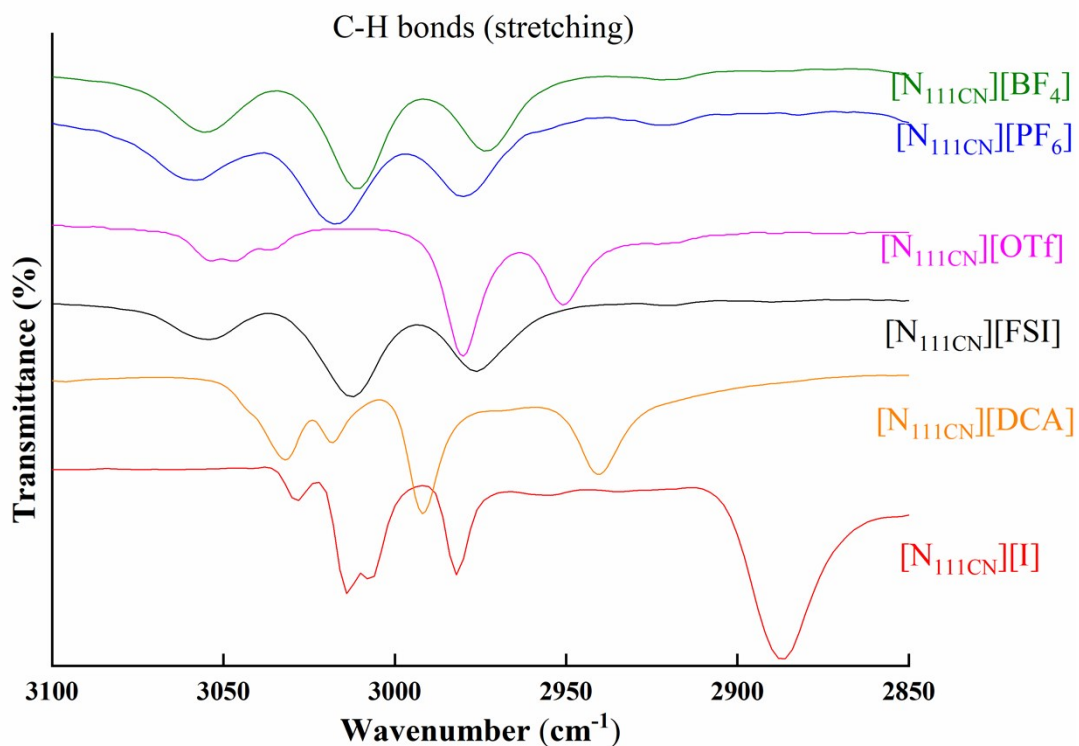


Figure S6. FTIR spectra for synthesized cyano-ammonium salts. Y-axis was adjusted for clarity.

Table S4: Names and acronyms for cations and anions discussed in the main text

Name of cation	Acronym of cation
Lithium	Li
(Cyanomethyl)trimethylammonium	[N _{111CN}]
Tetramethylammonium	[N ₁₁₁₁]
Ethyl(trimethyl)ammonium	[N ₁₁₁₂]
Butyl(trimethyl)ammonium	[N ₁₁₁₄]
Triethyl(methyl)ammonium	[N ₁₂₂₂]
Tetraethylammonium	[N ₂₂₂₂]
1-Ethyl-3-methylimidazolium	[emim]
N-Ethyl-N-methylpyrrolidinium	[C ₂ mpyr]
N,N-Diethylpyrrolidinium	[C ₂ epyr]
N-Propyl-N-methylpyrrolidinium	[C ₃ mpyr]
N-Isopropyl-N-methylpyrrolidinium	[C _(i3) mpyr]
Hexamethylguanidinium	[HMG]
Isobutyl(trimethyl)phosphonium	[P _{111i4}]
Tri(isobutyl)methylphosphonium	[P _{1i444}]
Isobutyl(diethyl)methylphosphonium	[P _{122i4}]
Polyvinylidene fluoride	PVDF
Name of anion	Acronym of anion
Bis(trifluoromethanesulfonyl)imide	[NTf ₂]

Bis(fluorosulfonyl)imide	[FSI]
Tetrafluoroborate	[BF ₄]
Hexafluorophosphate	[PF ₆]
dicyanamide	[DCA]
Iodide	[I]
Triflate	[OTf]
1,1,2,2,3,3-Hexafluoropropane-1,3-disulfonamide	[CPFSA]

Table S5. Ionic conductivity and parameters for the calculation of transference numbers for 50 mol% LiBF₄-[N_{111CN}][BF₄] electrolytes

	$\sigma^*/\text{S cm}^{-1}$	R_{i0}/Ω	R_{is}/Ω	I_0/A	I_s/A	t_{Li^+}
80 °C	3.0×10^{-5}	2399.1	2289.4	3.97×10^{-6}	1.77×10^{-6}	0.04
90 °C	0.78×10^{-3}	302.6	304.2	16.31×10^{-6}	6.88×10^{-6}	0.27

* Electrolyte conductivity extracted from Fig. 5d

References

1. M. Egashira, S. Okada, J.-i. Yamaki, D. A. Dri, F. Bonadies and B. Scrosati, *Journal of Power Sources*, 2004, **138**, 240-244.
2. M. Moriya, T. Watanabe, S. Nabeno, W. Sakamoto and T. Yogo, *Chemistry Letters*, 2014, **43**, 108-110.
3. Y. Zhou, X. Wang, H. Zhu, M. Yoshizawa-Fujita, Y. Miyachi, M. Armand, M. Forsyth, G. W. Greene, J. M. Pringle and P. C. Howlett, *ChemSusChem*, 2017, **10**, 3135-3145.
4. D. Al-Masri, R. Yunis, A. F. Hollenkamp and J. M. Pringle, *Chemical Communications*, 2018, **54**, 3660-3663.
5. H. Yoon, P. C. Howlett, A. S. Best, M. Forsyth and D. R. MacFarlane, *Journal of Electrochemical Society*, 2013, **160**, A1629-A1637.
6. G. M. A. Girard, M. Hilder, H. Zhu, D. Nucciarone, K. Whitbread, S. Zavorine, M. Moser, M. Forsyth, D. R. MacFarlane and P. C. Howlett, *Physical Chemistry Chemical Physics*, 2015, **17**, 8706-8713.
7. D. Al-Masri, R. Yunis, A. F. Hollenkamp, C. M. Doherty and J. M. Pringle, *Physical Chemistry Chemical Physics*, submitted.
8. H. Yoon, A. S. Best, M. Forsyth, D. R. MacFarlane and P. C. Howlett, *Physcial Chemistry Chemical Physcis*, 2015, **17**, 4656-4663.
9. G. M. A. Girard, M. Hilder, D. Nucciarone, K. Whitbread, S. Zavorine, M. Moser, M. Forsyth, D. R. MacFarlane and P. C. Howlett, *The Journal of Physical Chemistry C*, 2017, **121**, 21087-21095.